High-aspect-ratio metal microchannel plates for microelectronic cooling applications

2010 J. Micromech. Microeng. 20 025004

(http://iopscience.iop.org/0960-1317/20/2/025004)

J. Micromech. Microeng. 20 (2010) 025004 (8pp) doi:10.1088/0960-1317/20/2/025004

High-aspect-ratio metal microchannel plates for microelectronic cooling applications

W Yu[1], M P Y Desmulliez[2], A Drufke[2], M Leonard[2], R S Dhariwal[2], D Flynn[2], G Bognár[3], A Poppe[3], G Horvath[3], Z Kohari[3] and M Rencz[3]

[1] State Key Laboratory of Applied Optics, Changchun Institute of Optics, Fine Mechanics & Physics, Chinese Academy of Sciences, No. 3888, Dongnanhu Road, Changchun, Jilin, People's Republic of China

[2] Micro Systems Engineering Centre (MISEC), School of Engineering & Physical Sciences, Heriot-Watt University, Edinburgh EH14 4AS, UK

[3] Department of Electron Devices, Budapest University of Technology & Economics, H-1111 Budapest, Goldmann Gy. tér 3., Hungary

E-mail: yuweixing@pmail.ntu.edu.sg

Received 3 September 2009, in final form 20 November 2009
Published 15 December 2009
Online at stacks.iop.org/JMM/20/025004

Abstract

A new manufacturing process and the characterization of high-aspect-ratio metal microchannel plates for microelectronic cooling applications are reported in this article. A nickel-based microchannel cooling plate, with channels of width 20 μm and aspect ratio up to 3.6:1, has been successfully fabricated using a modified UV-LIGA process. Similar metal microstructures, based on electroplated copper, have also been obtained with a width of 15 μm and an aspect ratio of up to 5:1. In both cases, an over-plate technology was used to electroform the metallic microchannel plates in a single manufacturing step. Hydrodynamic and cooling characteristics of the microchannel plates such as flow rate and heat resistance have been measured. A heat transfer coefficient of 511 W m^{-2} K^{-1} for a flow rate of 120 l h^{-1} has been obtained for the 20 μm wide nickel-based microchannel.

(Some figures in this article are in colour only in the electronic version)

1. Introduction

Microelectronics cooling based on the use of microchannels has received considerable attention over the last 30 years since the seminal work of Tuckerman and Pease [1–3]. The understanding of the heat transfer in microchannels using single-phase or two-phase flow has also increased manifold [4] with gas and liquid single-phase flows investigated intensively [5, 6]. On the fabrication side, microchannels have been manufactured using various materials, but silicon predominantly, either wet or dry etched for small microchannels whereas large channels, mostly based on metal, have either been laser ablated or electrodeposited. An example of such a microchannel plate as part of a cooling system is provided in figure 1.

The UV-LIGA process offers an alternative approach to fabricate metal-based microchannels with dimensions down to 10 μm. This cost-effective process can be carried out at wafer scale and be adapted even to reel-to-reel manufacturing. Kim *et al* report the fabrication of metal-based radiant microchannels using electroforming [7]. In their work, the width of the microchannel ranges from 5 to 8 μm and the height ranges from 8 to 10 μm; thus, the aspect ratio is not more than 2. In [8, 9], Pang *et al* and Yu *et al* report nickel-based radiant microchannel cooling plates fabricated by the UV-LIGA process. The fabricated microchannels have a width of 100 μm and a depth of 70 μm and thus an aspect ratio of less than 2. In order to achieve a high-aspect-ratio microchannel by electroforming, thick photoresist should be used. In [8, 9], researchers use a positive tone photoresist AZ9260, which offers a film thickness of more than 20 μm for a single layer. However, to achieve a film thickness larger than 60 μm, a double layer process is normally needed which is complicated

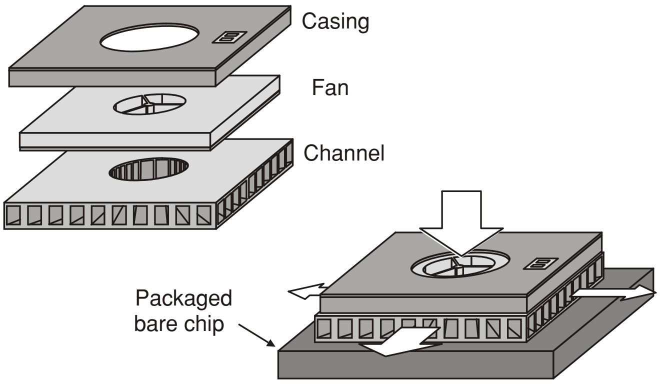

Figure 1. The microchannel cooling plate as part of a cooling system for microelectronics. The microfan shown here provides the assisted convection cooling.

and tedious. The negative tone photoresist, SU8, can offer a film thickness of more than 100 μm or even thicker in one layer as well as a high aspect ratio. However, this photoresist is known to be very hard to remove after polymerization. Recently, Rao and his co-authors reported another negative tone photoresist, JSR THB151N [10], which they used for wafer bumping application. Bumps with a diameter of 50 μm and an aspect ratio of 2.6 were achieved. This resist can be stripped easily as the polymerized photoresist can be totally dissolved in its stripper. In this paper, we demonstrate the fabrication of microchannels with a width of less than 20 μm and an aspect ratio of more than 3.6 in metallic materials of nickel and copper. The fabrication process described in this paper differs significantly from that in [8, 9] through the use of an over-plating process step and the creation of a very flat top surface that can be used for further processing. The fabricated microchannel plates have been designed for microelectronic cooling applications and their cooling characteristics have also been tested. A biomimetic design for one of the prototypes has also been manufactured with promising results as far as its hydrodynamic performance is concerned.

The layout of this paper is as follows. Section 2 describes the design of two microchannel plates that have been manufactured. Lengths, widths and number of channels of the two plates are presented with a particular emphasis on the second design that uses biomimetic principles to reduce energy losses within the channels. The microfabrication process stages are provided in section 3 alongside SEM photographs of the resulting plates. The characterization of the microchannels in terms of hydrodynamic and thermal capabilities is given in section 4. Conclusions are finally provided in section 5.

2. Design of the microchannel cooling plates

A schematic of the most significant parts of the microchannel cooling plates is shown in figure 2. Both configurations, a square plate of length 15 mm, have a hole at the centre of 6 mm diameter, which allows the input of the coolant during the cooling test. The type-I design, shown on the left-hand side of figure 2, encompasses 384 channels of 20 μm width, each of them radiating from the centre outwards. The right picture in figure 2 shows a configuration inspired from biomimetic principles. For a symmetric bifurcation, the first branch is split into two channels, which, for a circular cross-section, would obey Murray's law [11]. This law states that the sum of the cubes of the diameters of bifurcated similar channels is equal to the cube of the diameter of the original channel. More generally, ${D_0}^3 = 2^n {D_n}^3$, with $n = 1, 2, 3$, where D_0 is the mother channel and D_n represents the nth generation of the microchannel. Such a relation, named Murray's law, has been demonstrated to generate the minimum energy loss and constant shear stress throughout the whole microfluidic network [11]. The relation provided above cannot be applied directly in the calculation of the width of microchannels whose cross-section is rectangular. Accordingly, the formula needs to be modified for more general cases, following the work carried out by Emerson *et al* [12]. The application of Murray's law to the microchannel with a rectangular cross-section in our case leads to the following equations [12]:

$$\alpha_n(1+\alpha_n)\mathrm{P_O}(\alpha_n^*) = 2^n\alpha_0(1+\alpha_0)\mathrm{P_O}(\alpha_0^*) \tag{1}$$

$$\mathrm{P_O}(\alpha_n^*) = 24[1 - a_1\alpha_n^* + a_2(\alpha_n^*)^2 - a_3(\alpha_n^*)^3 + a_4(\alpha_n^*)^4 - a_5(\alpha_n^*)^5], \tag{2}$$

where $\alpha_n = d/w_n$ is the aspect ratio of the nth generation, d and w_n are the depth of the microchannel and the width of the nth generation, respectively, and $\mathrm{P_O}$ is the Poiseuille number. It should be noted that both equations above require that $\alpha_n^* \leqslant 1$, which implies that the aspect ratio should be not more than 1:1, and thus $\alpha_n^* = \alpha_n = d/w_n$; if the aspect ratio

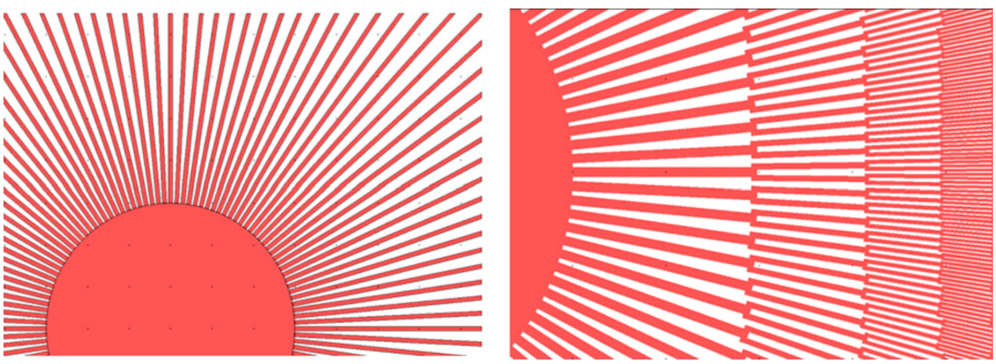

Figure 2. Type-I microchannel (left) and biomimetic-type microchannel (right).

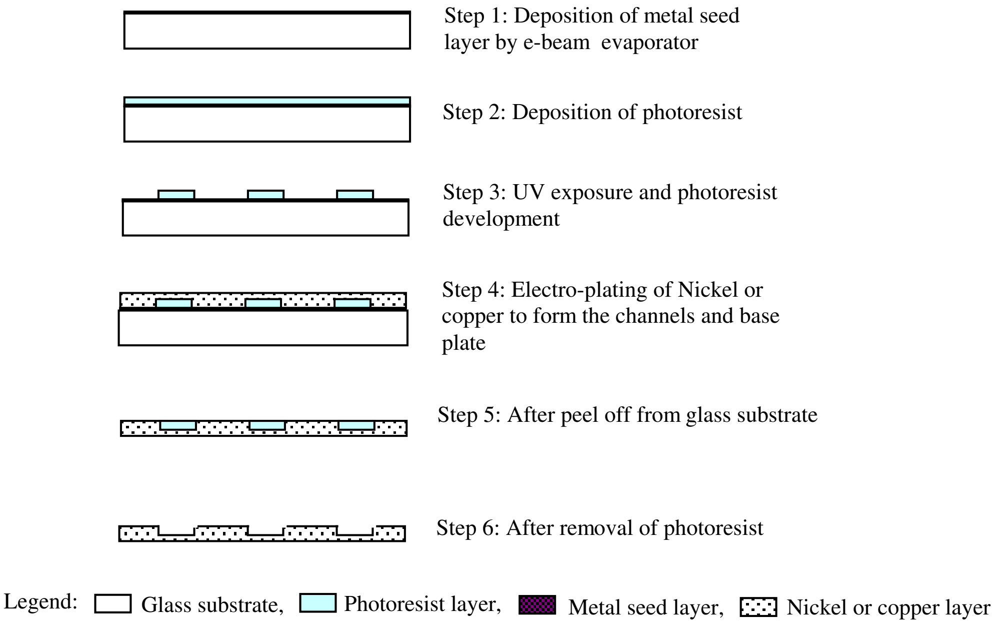

Figure 3. Process flow for the manufacturing of the microchannel cooling plate.

Table 1. Design parameters of the biomimetic-type microchannel cooling plate.

Branch no		1	2	3	4
Width of each channel		100 μm	62 μm	41 μm	28 μm
Total number of channels		128	256	512	1024
Length of channels	Shortest	1.95 mm	1.21 mm	0.80 mm	0.55 mm
	Longest	4.59 mm	2.85 mm	1.86 mm	1.29 mm

is larger than 1:1, then $\alpha_n^* = w_n/d$. The required coefficients in equation (2) are $a_1 = 1.3553$, $a_2 = 1.9467$, $a_3 = 1.7012$, $a_4 = 0.9564$ and $a_5 = 0.2537$, respectively. For convenience, we set $\alpha_0 = 0.7$, which means the mother channel has a width of 100 μm and the depth is always 70 μm throughout the whole microchannel plate. By solving the above equations, the width of the microchannel for each branching generation can be obtained. The length of the microchannel of each generation is determined by considering the proportion of its width to the sum of the width of all the channels, which means the larger the width, the longer the channel. Since the channel length varies for the entire plate, we give only the shortest and the longest channel length. As a result, in our design, each channel is split into two channels and each original channel generates eight channels at the perimeter of the cooling plate through three stages of splitting. The detailed design parameters for this type of configuration are presented in table 1. Only four levels of branching are chosen in the design due to the manufacture limitation for our current UV-LIGA process. For the current four-branch design, the minimum width of the microchannel is 28 μm and the space between the microchannel is as narrow as 15 μm (aspect ratio 5:1), which is already difficult to manufacture for the UV-LIGA process. Further improvement of the manufacturing process, such as using the overlap photoresist technology to increase the aspect ratio of the microchannels further, would be needed if further branching were deemed necessary.

3. Microfabrication process

The modified UV-LIGA process flow used for the fabrication of microchannels is represented schematically in figure 3. A metal seed layer is first deposited using e-beam evaporation on pre-cleaned glass wafers. The metal thin film acts as a seed layer for the subsequent electroforming process. Depending on the metal used during electroforming, two kinds of metal thin films, Ti/Cu with thickness of 100 nm/400 nm or Cu with a thickness of 400 nm, are deposited for nickel and copper plating, respectively. This odd choice of the seed layer is to guarantee that a poor adhesion exists at the different material interfaces such that the electroformed microchannel cooling plate can be easily released at the end of the manufacturing process. For nickel plating, the poor adhesion between the electroplated nickel microstructure and the metallic seed layer is achieved by using Ti/Cu/Ti but not Ti/Ni as the seed layer for nickel plating. It is well known that a vacuum-deposited Ti layer normally has a good adhesion to a glass substrate; however, the Ti layer has a poor adhesion to electroplated nickel if its surface is not descumed by plasma treatment after the photolithography process. Hence, after electroplating, the nickel plate can be easily peeled off from the Ti/Cu/Ti seed layer. For copper plating, the poor adhesion between the seed layer and the glass substrate is achieved by using Cu but not Ti/Cu as the seed layer. However, the electroplated copper plate has a good adhesion to the Cu seed layer. Hence, after electroplating, the copper plate can be easily peeled off from the glass substrate. In both cases, a copper layer is used as a good electric conductive layer to achieve a good plating result. It should be noted on the other hand that the poor adhesion should be avoided due to the film stress especially for the thick film which might lead to the peeling off of the film from the substrate during the electroplating process. However for our process, we found that the photoresist THB151N has a quite good adhesion to the substrate even for a film thickness of larger than 100 μm, and thus the photoresist is never found to peel off from the substrate. However, we did observe the peeling off or delaminating of the microchannel plate from the substrate during the electroplating when we used a higher current density of 30 mA cm^{-2}, which we attribute to the film stress accumulated in the plate during electroplating, and the poor adhesion of the film cannot hold firmly the microchannel plate onto the substrate. However, we find if we use a lower current density of around 5 mA cm^{-2}, the electroplated microchannel plate has a better rigidity and the film stress accumulated in the film is reduced significantly so that the film will not peel off or delaminate from the substrate during the electroplating process.

The second step is the spin coating of the thick negative tone photoresist film JSR THB151N onto the substrate. This resist has a high viscosity of 3000 cts so that a thickness of up to 100 μm can be easily deposited by one layer spinning. Specifically for this work, a film thickness of 60 μm is achieved by a spinning speed of 1000 rpm for 15 s and followed by a soft baking at 120 °C for 40 min. A film thickness of 70 μm can be obtained by a spinning speed of 1000 rpm for 10 s followed by a soft baking at 120 °C for 20 min. As the ratio of length to width of the channel is up to 380:1, an optimum soft-baking time needs to be found out in order to remove as much solvent as possible during baking. Otherwise, the remained solvent will help the developer lift off the long webs between microchannels during the development process. Unlike positive photoresist, a rehydration process is not needed before exposure for this negative tone photoresist. Once the photoresist has been cooled down to room temperature, it can be exposed immediately with a broadband UV light. The exposure energy in step 3 is 800 mJ cm^{-2} for 60 μm and 1000 mJ cm^{-2} for 70 μm thick film.

The electroplating process in step 4 is voluntarily extended such that the channels are over-electroformed. This over-plating process permits the creation of the base plate. There are several advantages of this process. Firstly, the adhesion between the channel layer and base plate is very strong, as both features are formed from the same material continuously. Secondly, the uniformity of the channel depth is very good and depends on the uniformity of the thickness of the photoresist. Finally, by plating first the top of the microchannels in this inverted process flow, a flat top surface is guaranteed which allows a very close contact with the electronic die during subsequent assembly of the cooling system. A current density of 15 mA cm^{-2} and a plating time of 20 h were used for the nickel plating of 60 μm deep microchannels. After plating, in step 5 the device can be easily peeled off from the substrate as the Ti/Cu seed layer has poor adhesion with the nickel-based electroformed channels. A stripper named EKC108 was used in step 6 to strip the photoresist by soaking the plated device in stripper at a temperature of 65 °C for 1 h.

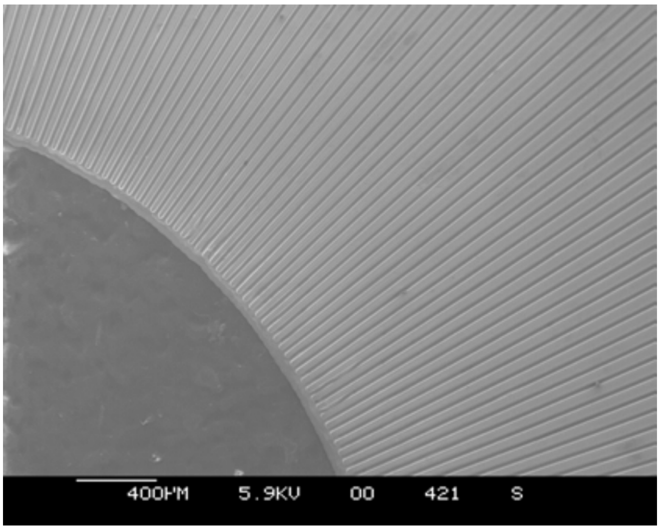

Figure 4. SEM image of part of the fabricated microchannel cooling plate with a width of 20 μm and a depth of 60 μm.

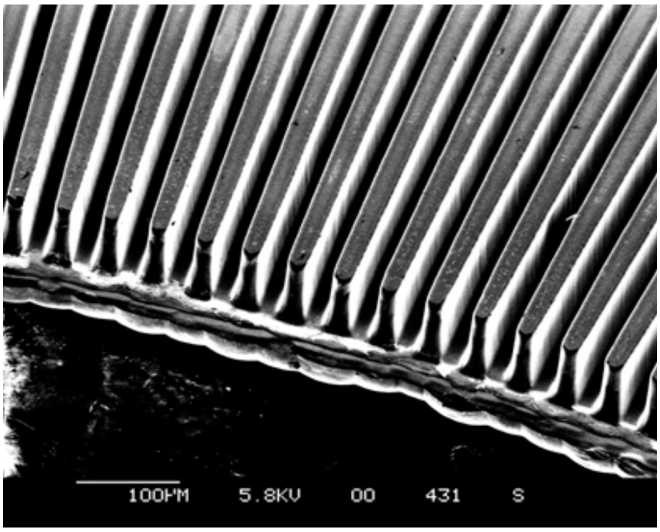

Figure 5. Cross-section SEM image of the 20 μm wide microchannel.

In the copper plating case, a seed layer of copper is deposited on a pre-cleaned glass substrate to make ease of the release of the electroformed microchannel plate from the substrate. The same photolithography process is used to pattern the microchannels following the biomimetic design. A small current density of 6 mA cm^{-2} is used during the plating so that a structure of as small as 15 μm channel width and an aspect ratio up to 5:1 can be electroformed.

Figure 4 shows the SEM picture of the fabricated microchannel cooling plate with 384 channels. Each channel has a width of 20 μm and a depth of 60 μm. The channel width is very uniform with an average of 19.8 μm, which is very close to the designed width of 20 μm. Figure 5 shows the cross-section of the microchannels whose sidewalls appear straight and smooth. By using the above fabrication process,

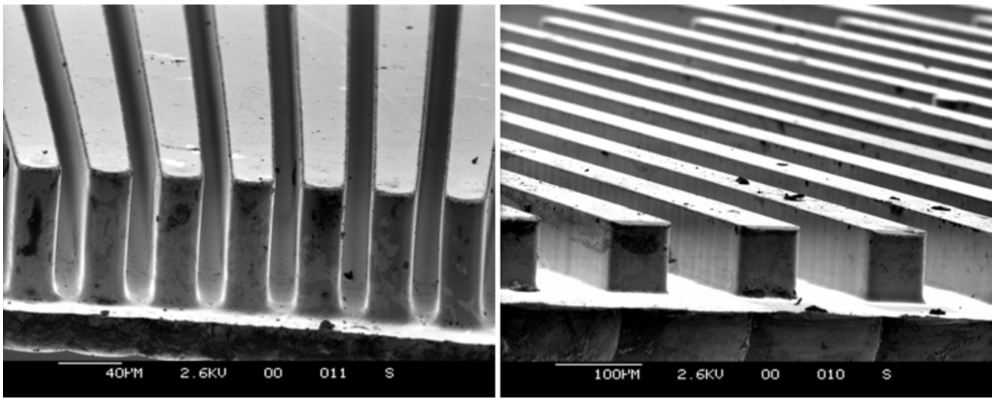

Figure 6. SEM pictures of the microchannel with a width of 20 μm and an aspect ratio of 3.6:1 (left), and a width of 100 μm and an aspect ratio of 0.7:1 (right).

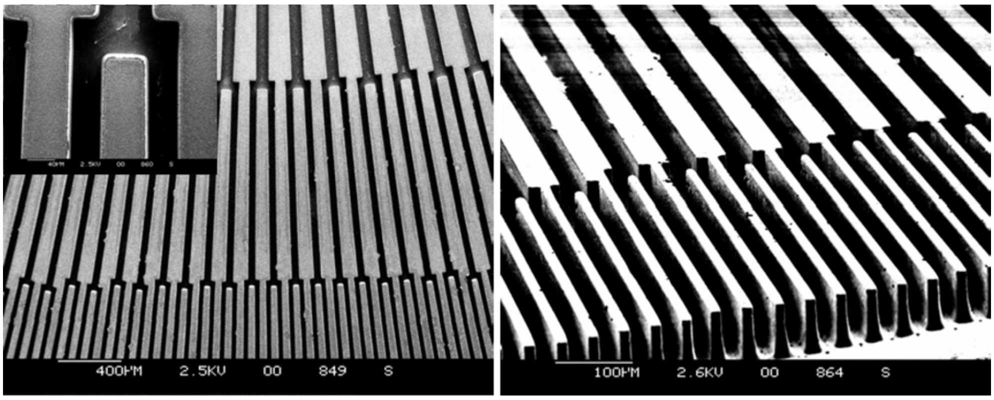

Figure 7. SEM pictures of the copper-based microchannels using the biomimetic design.

microchannels with channel widths ranging from 100 μm down to 20 μm and aspect ratio from 0.7:1 to 3.6:1 have also been fabricated in nickel as shown in figure 6. The top surface of the electroformed structures is very flat and the roughness is only limited by the grain size of the nickel crystal formed in electroplating. The sidewall is also quite straight with a wall angle of nearly 90°. A small slop at the bottom of the sidewalls of the 20 μm wide microchannels can be noticed. This slop stems from the top sidewalls of the photoresist moulds attacked by the developer during the long time development process. Such a small slop does not appear for the wider channels. This slop issue can be improved by optimizing the soft-baking time and the exposure energy so that the exposed photoresist is strong enough to resist the attack from the developer solution.

Figure 7 shows the copper-based manufactured microchannel plate that uses the biomimetic design. A current density as small as 6 mA cm^{-2} during electroplating is used to ensure that the smallest features can be manufactured. The left picture shows the different bifurcation branches while the right picture shows the cross-section image of the microchannels near the outside perimeter of the channel plate. Here the fin of the microchannel has a width of only 15 μm. As the height of the fin is 75 μm, the actual aspect ratio of the fin formed by copper electroplating is 5:1. The sidewall of the microchannel as well as the top surface is not as smooth as that obtained by nickel plating due to the bigger grain size of the copper crystal. This grain size could be reduced by modifying the copper plating solution through the addition of surfactant additives.

4. Characterization of the microchannel plate

The microchannel cooling plate was characterized in terms of flow rate and thermal resistance. The schematic diagram of the experimental setup used to measure the flow rate of the microchannel cooling plate is shown in figure 8. Basically compressed nitrogen was used as the gas coolant; the pressure drop and the flow rate in the supplying tube were monitored in real time. The microchannel plate was mounted on a glass substrate with the channels facing towards the substrate and a tube was mounted vertically on the top of the cooling plate. A rubber 'O' ring was used to make sure the intimate contact between the tube and the cooling plate. The gas was injected into the microchannel through the centre hole and exits from the end of the microchannels. The detailed description of this setup and the flow rate characterization can be found in [8].

Figure 9 shows the measured flow velocity against pressure for the fabricated microchannel plates. For the same pressure drop, the biomimetic microchannel plate has a higher flow velocity than the type-I microchannel plate. For the two

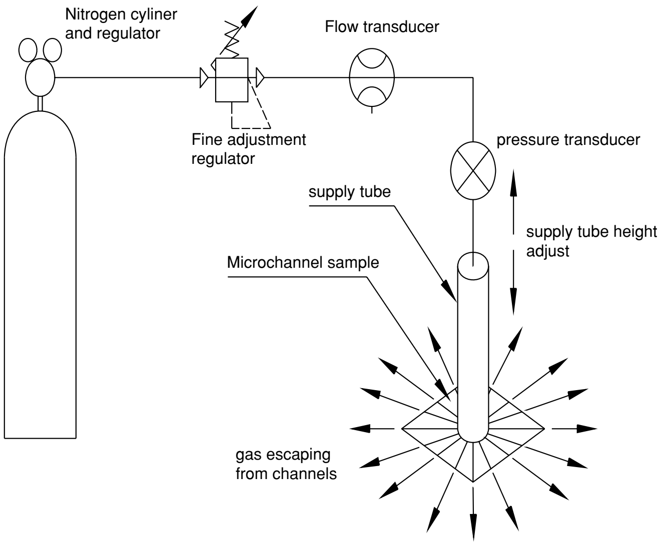

Figure 8. Schematic diagram of the experiment setup for measuring the flow rate of the microchannel cooling plate.

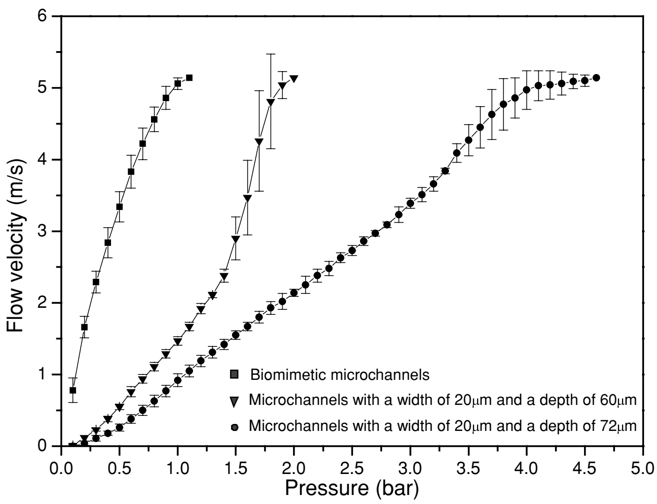

Figure 9. Flow velocity of microchannel cooling plates against pressure.

type-I plates, the higher the aspect ratio of the channel, the lower the flow velocity for the same pressure drop. Also, for a pressure drop of 2 bars, the slight increase of the aspect ratio of the channel from 0.6:1 to 0.72:1 causes a 58% drop of flow velocity. As the depth difference for the channels in the two types of plates is 12 μm, or about 60% of the channel width, the aspect ratio affects significantly the flow rate.

In reference to our previous work [8, 9, 13], the flow characterization results show that high-aspect-ratio (>3:1) type-I microchannels need a higher pressure drop in order to achieve the same flow velocity as with the previously reported low-aspect-ratio (0.7:1) microchannel plate. However, although biomimetic-type microchannels have a high aspect ratio (from 0.7:1 to 2.6:1), the same pressure drop as in our first designs is needed to achieve the same flow velocity. In practice, low pressure drop is always preferred. Thus, the biomimetic-type microchannel plate requires, for a given flow rate, less power to achieve the required pressure drop.

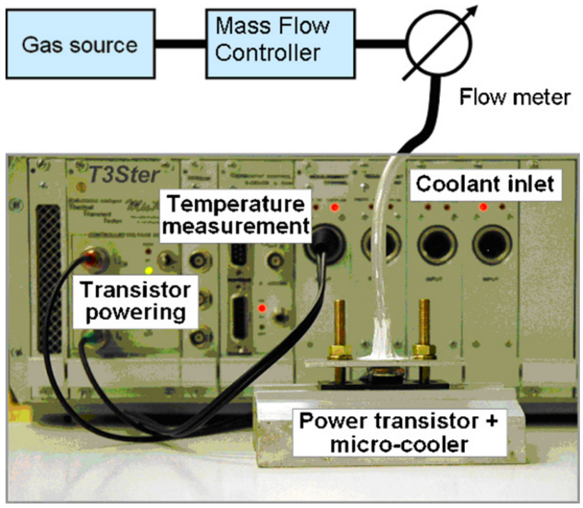

Figure 10. Schematic view of the thermal transient measurement setup.

To characterize the cooling capability of the channel plate, the thermal resistance was measured by the T3Ster thermal transient tester equipment [14]. Figure 10 shows the schematic view of the thermal transient measurement setup, in which the micro-cooling plate is attached to a heat-dissipating element. A flat surface copper plate of $15 \times 15 \times 2$ mm^3 was used as a heat spreader. The micro-cooler is mounted such that the channels face the flat copper plate. The gas supply tube, seamlessly joined to a silicone rubber sheet, ensures the cooling gas flow to the central hole. The rubber sheet protects the micro-cooler plate from breaking. A detailed explanation of the principles of thermal transient measurement can be found in [15].

Figures 11 and 12 show the measured differential structure functions and cumulative structure functions for a 20 μm wide microchannel cooling plate and biomimetic-type microchannel cooling plate, respectively, at different flow rates. From both figures, one can see that the higher the flow rate, the lower the thermal resistance and thus the higher the cooling efficiency. The 20 μm wide microchannel cooling plate has the lowest thermal resistance, 10 K W^{-1}, due to its largest surface area formed by the high-aspect-ratio (3:1) microchannels over the entire plate. For the biomimetic-type microchannel cooling plate, the thermal resistance is 12.2 K W^{-1}, which is lower than that of the 20 μm wide microchannel cooling plate due to the relatively lower surface area formed by the variable aspect ratio of microchannels, which is 0.7, 1.1, 1.7 and 2.5 for branches 1 to 4, respectively. In addition, the characteristic change of the flow pronounced by the peaks in the plots for the 20 μm wide microchannel can be seen at both 60 l h^{-1} and 120 l h^{-1} flow rates, while this phenomenon only occurs at a flow rate of 120 l h^{-1} for biomimetic microchannels. Obviously, this change of flow should be avoided as it changes the trend of the curve abruptly to make the thermal resistance larger than it should be. However, for both the 20 μm wide type-I and biomimetic-type microchannels, a lower thermal resistance and thus a higher cooling efficiency than the previous 100 μm wide type-I microchannel has been demonstrated.

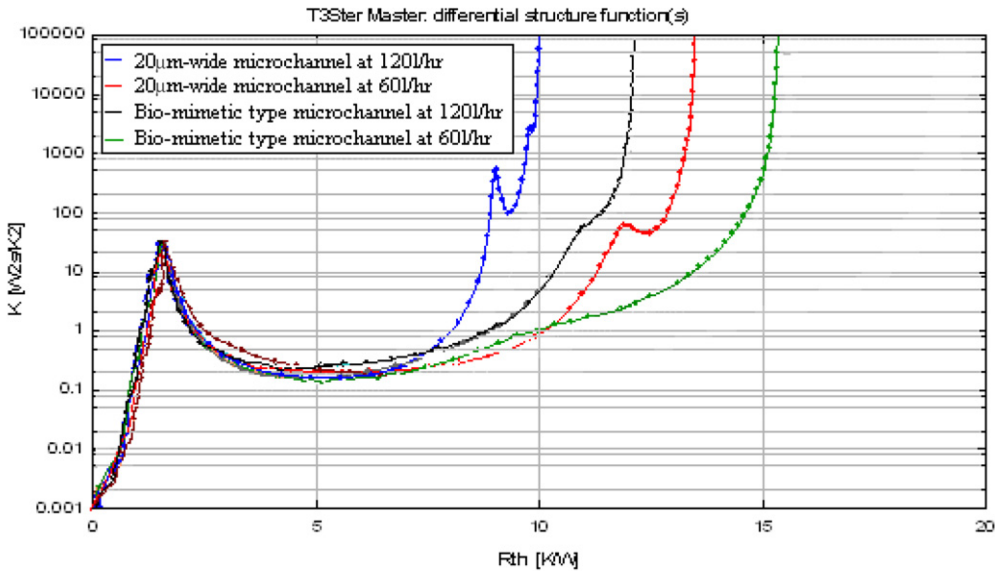

Figure 11. Differential structure functions of the 20 μm wide type-I microchannel and biomimetic-type microchannel cooling plates at flow rates of 60 l h^{-1} and 120 l h^{-1}.

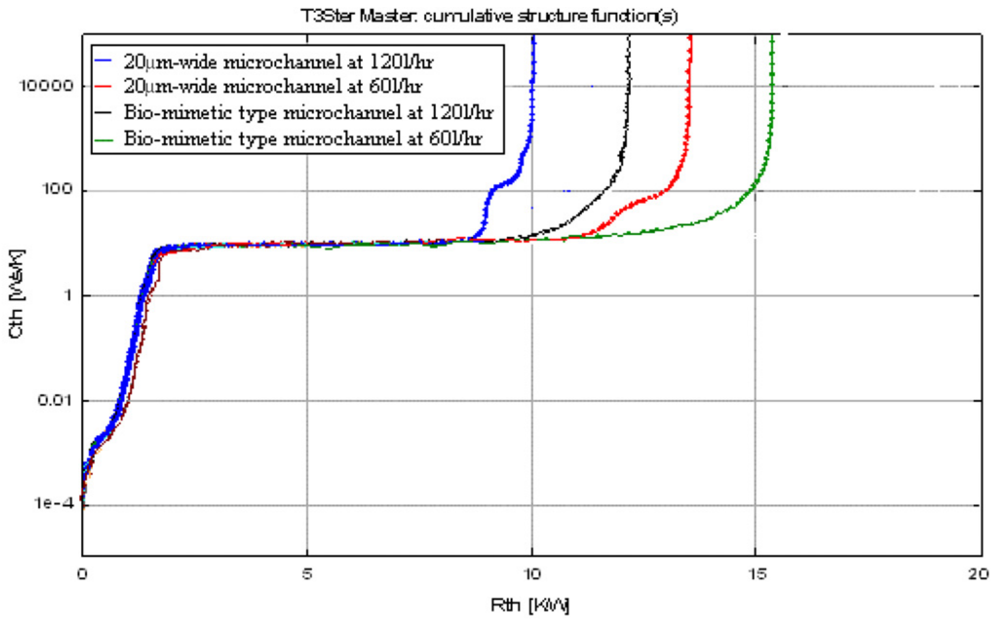

Figure 12. Cumulative structure functions of the 20 μm wide type-I microchannel and biomimetic-type microchannel cooling plates at flow rates of 60 l h^{-1} and 120 l h^{-1}.

Once the thermal resistance of the microchannel cooling plate is known, the heat transfer coefficient can be calculated by the following formula [16]:

$$\lambda = 1/(rA), \tag{3}$$

where λ, r and A are the heat coefficient, thermal resistance and cross-section area of the microchannel cooling plate, respectively. By applying the above formula, the heat transfer coefficients of the 20 μm wide type-I and biomimetic-type microchannels were calculated as 511 W m^{-2} K^{-1} and 417 W m^{-2} K^{-1}, respectively, at a flow rate of 120 l h^{-1}. Compared to previous low-aspect-ratio type-I microchannels reported in [8, 9, 13], the heat transfer coefficient is 70% and 39% higher for the 20 μm wide type-I microchannel and biomimetic-type microchannel, respectively, which shows a significant improvement in the cooling efficiency of the new design. We believe that a higher heat transfer coefficient could be further obtained by using a liquid coolant.

5. Conclusions

In conclusion, we have reported the UV-LIGA-based manufacturing of high-aspect-ratio metal-based microchannel plates using a single electroplating step. The negative tone photoresist, THB151N, was used to allow the fabrication of high-aspect-ratio microchannels (up to 3.6) whilst allowing the easy removal of the resist. The resulting fabricated microchannel plates have been hydrodynamically and thermally characterized through the measurement of flow rate and thermal resistance. The flow rate achievable has shown to be strongly dependent on the aspect ratio. Such microchannel plates offer interesting prospects in terms of microelectronic cooling performance especially as the manufacturing process described above could be directly carried out on the back of processed die or wafers.

Acknowledgments

The authors acknowledge funding from the British Engineering and Physical Sciences Research Council (EPSRC) through the 3D-Mintegration Grand Challenge project (EP/C534212/1). Financial contribution from the EEC Framework 6 Program is also acknowledged through the Network of Excellence DfMM PATENT, Design for Micro & Nano-Manufacture (contract number 507255), the INFOTERM NKFP-2/0018/2001 and the OTKA TS04989 projects of the Hungarian Government. Finally, the financial support from the Strategic Research Development Grant of the Scottish Funding Council is also gratefully acknowledged through the programme SCIMPS (Scottish Consortium in Integrated MicroPhotonic Systems).

References

[1] Tuckerman D B and Pease R F W 1981 High-performance heat sinking for VLSI *IEEE Electron Device Lett.* **2** 126–9
[2] Mundinger D, Beack R, Benett W, Solarz R, Sperry V and Ciarlo D 1990 High average power edge emitting laser diode arrays on silicon microchannel coolers *Appl. Phys. Lett.* **57** 2172–4
[3] Zhou P, Hom J, Upadhya G, Goodson K and Munch M 2004 Electro-kinetic microchannel cooling system for desktop computers *20th Annual IEEE Semiconductor Thermal Measurement and Management Symp. (San Jose, 9–11 March 2004)* pp 26–9
[4] Hassan I, Phutthavong P and Abdelgawad M 2004 Microchannel heat sinks: an overview of the state-of-the-art *Microscale Thermophys. Eng.* **8** 183–205
[5] Marongiu M J 1996 Compressibility effects in the design of gas-cooled microchannel heat sinks *Proc. 5th Intersociety Conf. on Thermal Phenomena in Electronic Systems* p 124
[6] Guo Z-Y and Li Z-X 2003 Size effect on single-phase channel flow and heat transfer at microscale *Int. J. Heat Fluid Flow* **24** 284–98
[7] Joo Youngcheol, Dieu Kiet and Kim Chang-Jin 1995 Fabrication of monolithic microchannels for IC chip cooling *Micro Electro Mechanical Systems: MEMS '95, Proc. IEEE (29 January 1995)* pp 362–7
[8] Pang A J *et al* 2004 Design, manufacture and testing of a low-cost micro-channel cooling device *IEEE Proc. of the 6th Electronics Packaging Technology Conf. (Singapore)* p 564
[9] Desmulliez M P Y *et al* 2009 Fabrication and characterization of a low-cost, wafer-scale radial microchannel cooling plate *IEEE Trans. Compon. Packag. Technol.* **32** 20–9
[10] Rao V S, Kripesh V, Yoon S W and Tay A A O 2006 A thick photoresist process for advanced wafer level packaging applications using JSR THB-151N negative tone UV photoresist *J. Micromech. Microeng.* **16** 1841–6
[11] Murray C D 1926 The physiological principle of minimum work *Proc. Natl. Acad. Sci. USA* **12** 207–14
[12] Emerson D R, Cieślicki K, Gu X and Barber R W 2006 Biomimetic design of microfluidic manifolds based on a generalised Murray's law *Lab on a Chip* **6** 447–54
[13] Kohári Zs, Bognár Gy, Horváth Gy, Poppe A, Rencz M and Székely V 2007 Cross-verification of thermal characterization of a microcooler *J. Electron. Packag.* **129** 167–71
[14] http://www.mentor.com/products/mechanical/products/t3ster
[15] Bognár Gy, Horváth Gy, Kohári Zs, Pang A J, Desmulliez M P Y, Poppe A, Rencz M and Székely V 2005 Thermal characterization of a radial micro-channel cooling plate *21st Annual IEEE Symp. on Semiconductor Thermal Measurement and Management* p 135
[16] Székely V 1997 A new evaluation method of thermal transient measurement results *Microelectron. J.* **28** 277–92